Electronic Supplementary Material (ESI) for New Journal of Chemistry.

Supplementary Information

Ammonium ion intercalation and oxygen-rich vacancies in birnessite-type MnO_2 for supercapacitor and oxygen evolution applications

Juyin Liu, Xiaoze Ren, Yanfang Gao, Ling Liu*, II*

**School of Chemical Engineering, Inner Mongolia University of Technology, Hohhot 010051, P. R. China*

Engineering Research Center of Large Energy Storage Technology

* E-mail addresses: *yf_gao@imut.edu.cn*

*, II E-mail addresses: *ll@imut.edu.cn*

Experimental Procedures

Chemicals and reagents

Potassium permanganate ($KMnO_4$) was purchased from Tianjin Damao Chemical Reagent Co., Ltd. Ammonium chloride (NH_4Cl) was purchased from Aladdin Reagent (Shanghai) Co., Ltd. Lithium sulphate (Li_2SO_4) was purchased from Aladdin Reagent (Shanghai) Co., Ltd. Nickel foam (NF) was purchased from Taiyuan Lizhiyuan Technology Co., Ltd. All reagents were directly used without further purification. All solutions were prepared using ultrapure water.

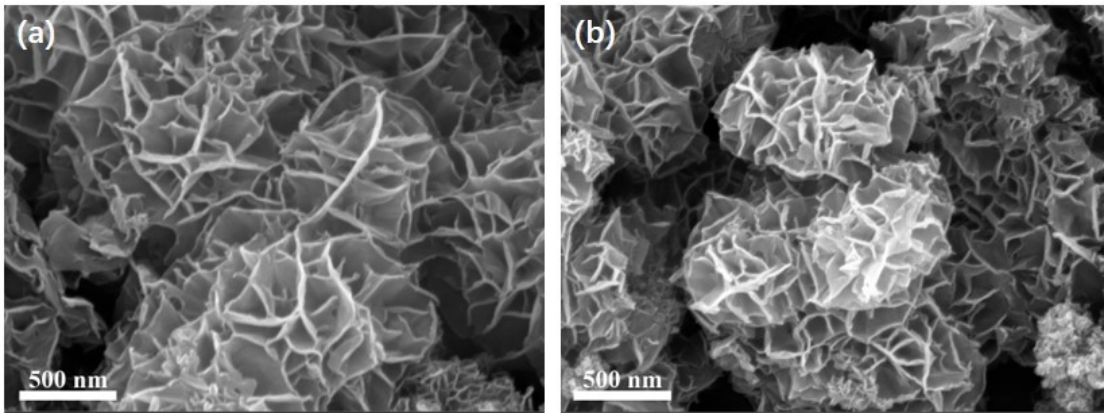

Fig. S1. SEM images of (a) 0.5 M-A-MnO_2. (b) 2 M-A-MnO_2.

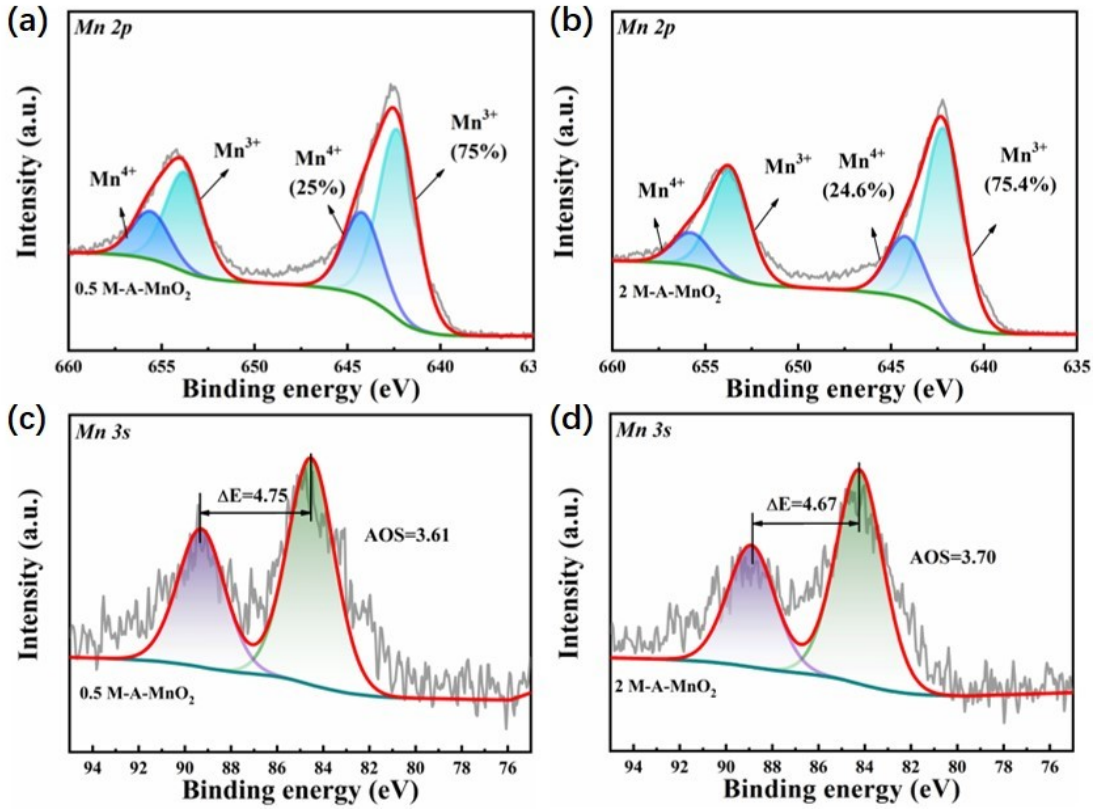

Fig. S2. (a-b) Mn 2p spectra of 0.5 M-A-MnO_2 and 2 M-A-MnO_2. (c-d) Mn 3s spectra of 0.5 M-A-MnO_2 and 2 M-A-MnO_2 samples.

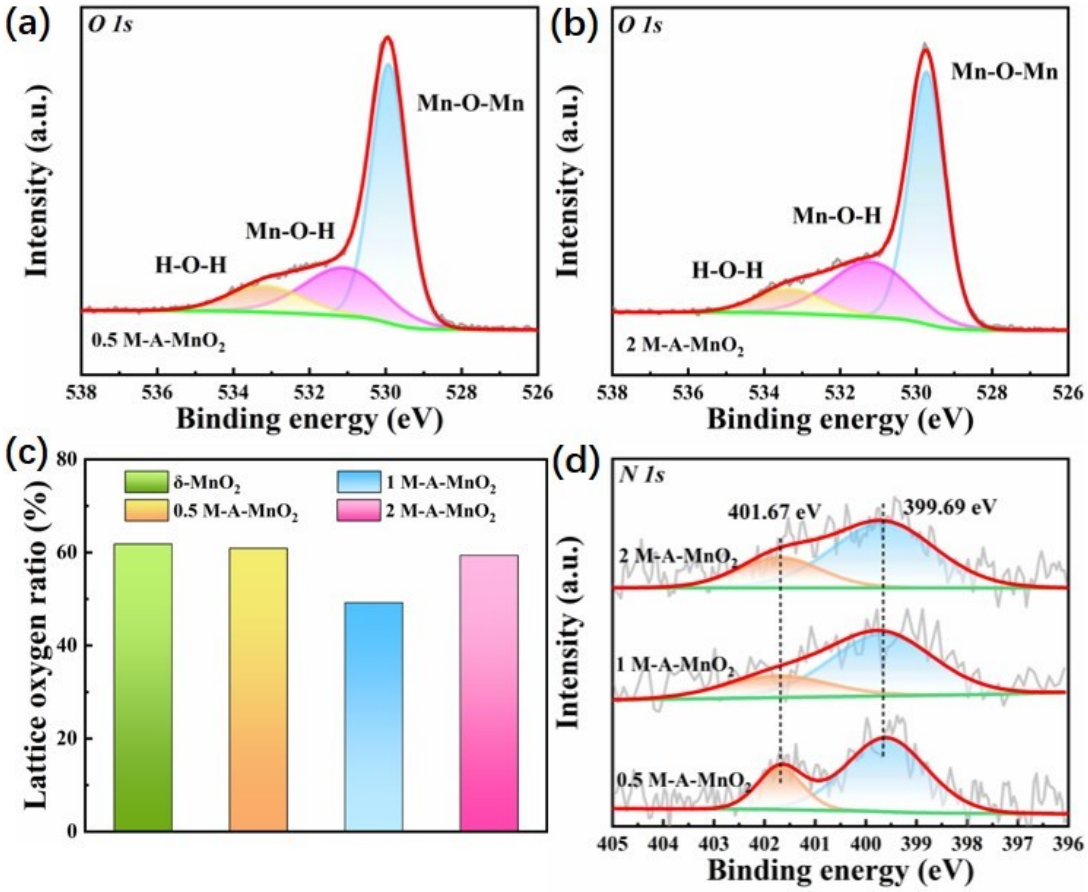

Fig. S3. (a-b) O 1s spectra of 0.5 M-A-MnO_2 and 2 M-A-MnO_2. (c) Ratio of lattice oxygen concentrations for four samples. (d) N 1s spectra of C-A-MnO_2.

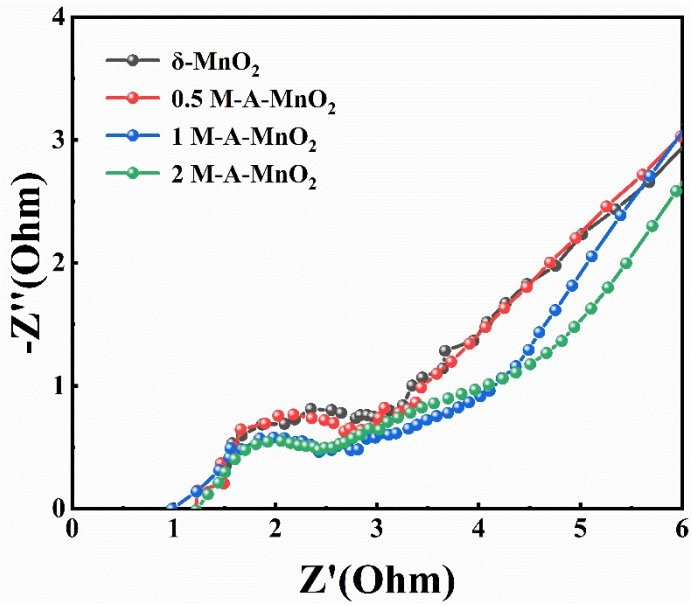

Fig. S4. Local magnification of the C-A-MnO_2 impedance spectra.

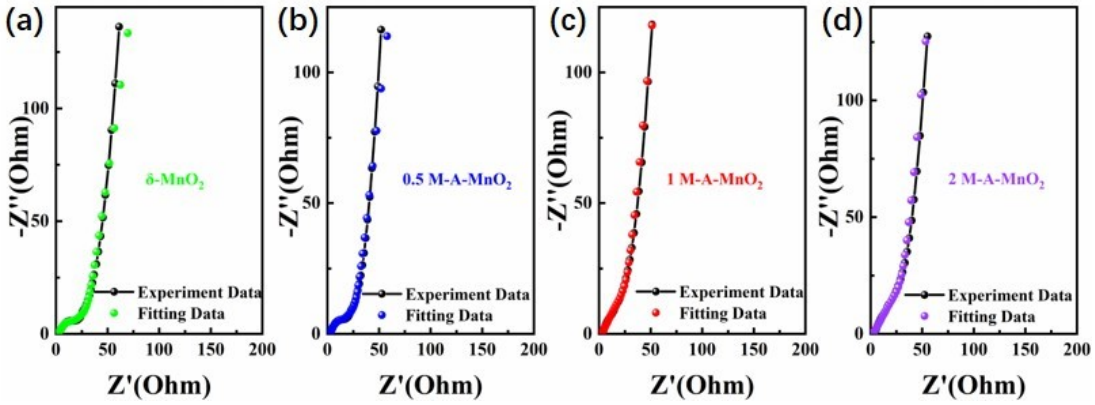

Fig. S5. Impedance fitting results of the C-A-MnO_2.

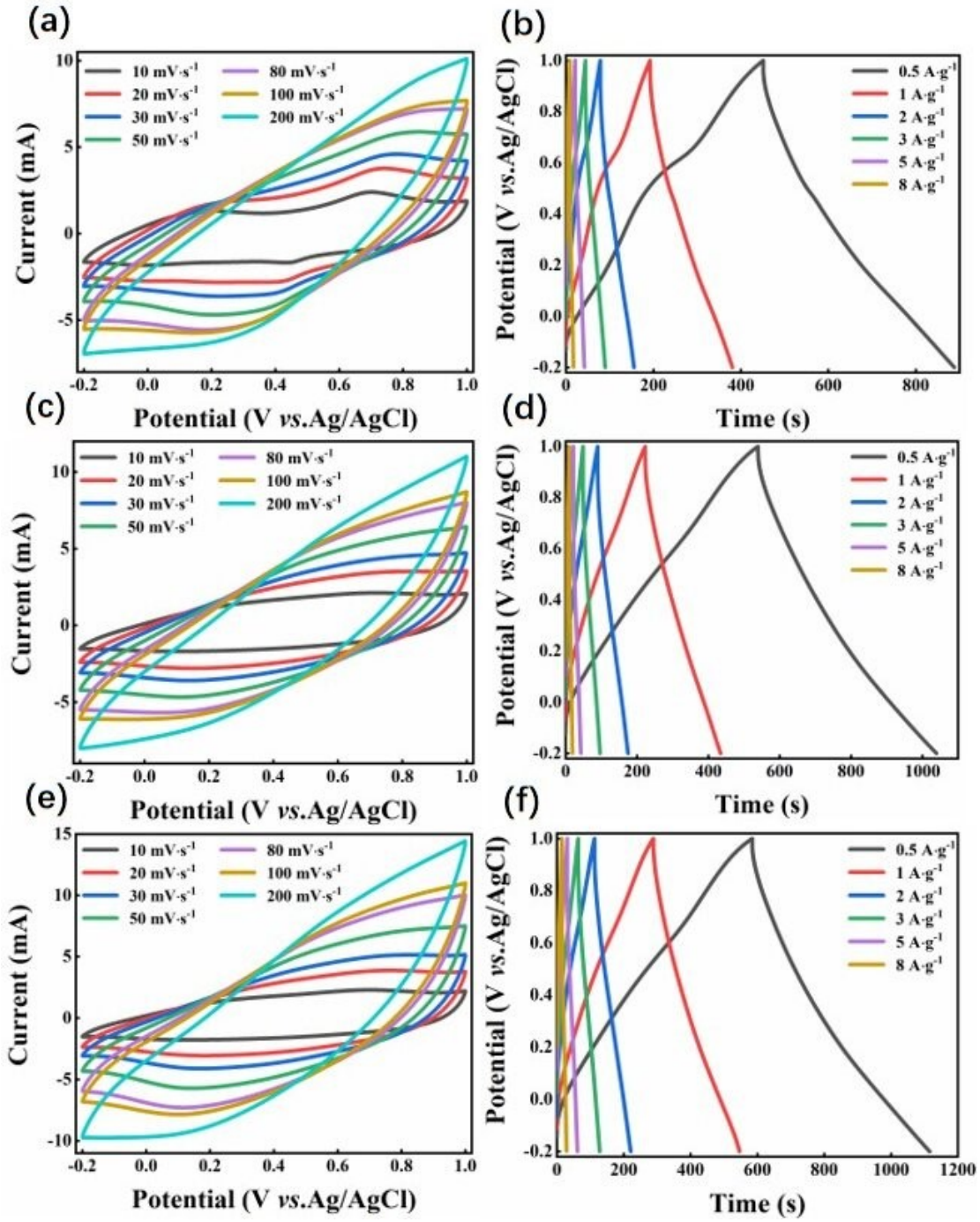

Fig. S6. (a) CV and GCD curves of three samples: (a, b) δ-MnO_2. (c, d) 0.5 M-A-MnO_2. (e, f) 2 M-A-MnO_2.

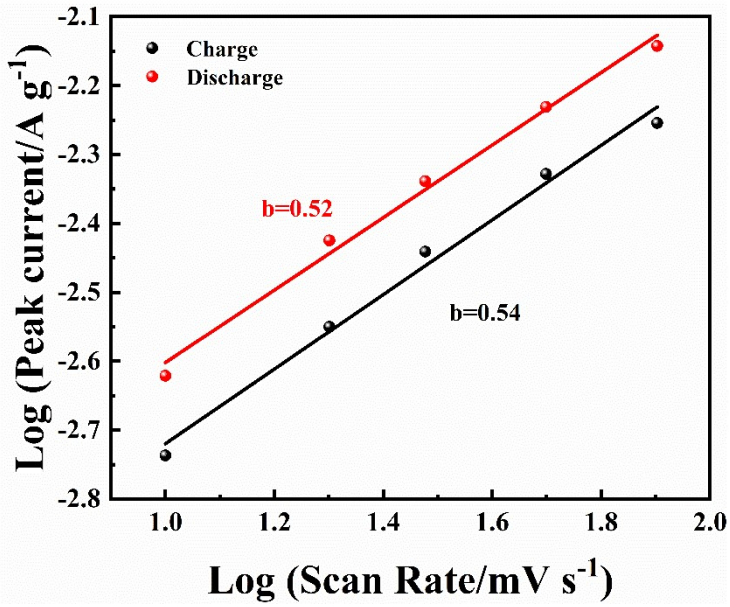

Fig. S7. The linear fitting curves of log (i) vs log (ν) according to the CV results in Fig. S6. (a).

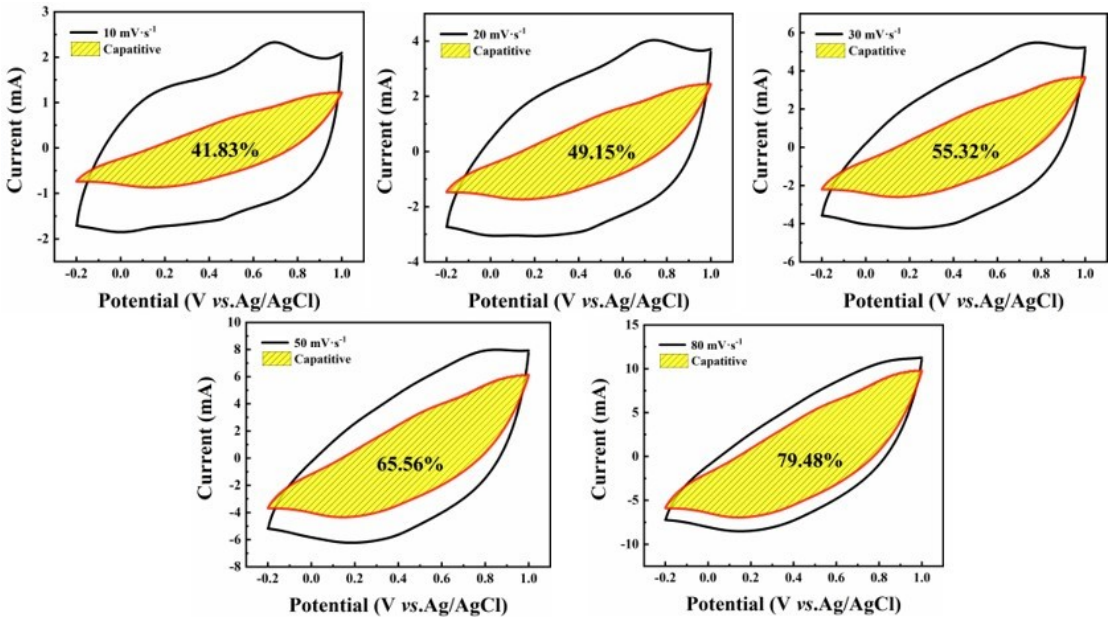

Fig. S8. Pseudocapacitive fraction (shown by the shaded area) calculated at a scan rate of 10-80 mV s^{-1} from CV curves at different scan rates of A-MnO_2 electrode.

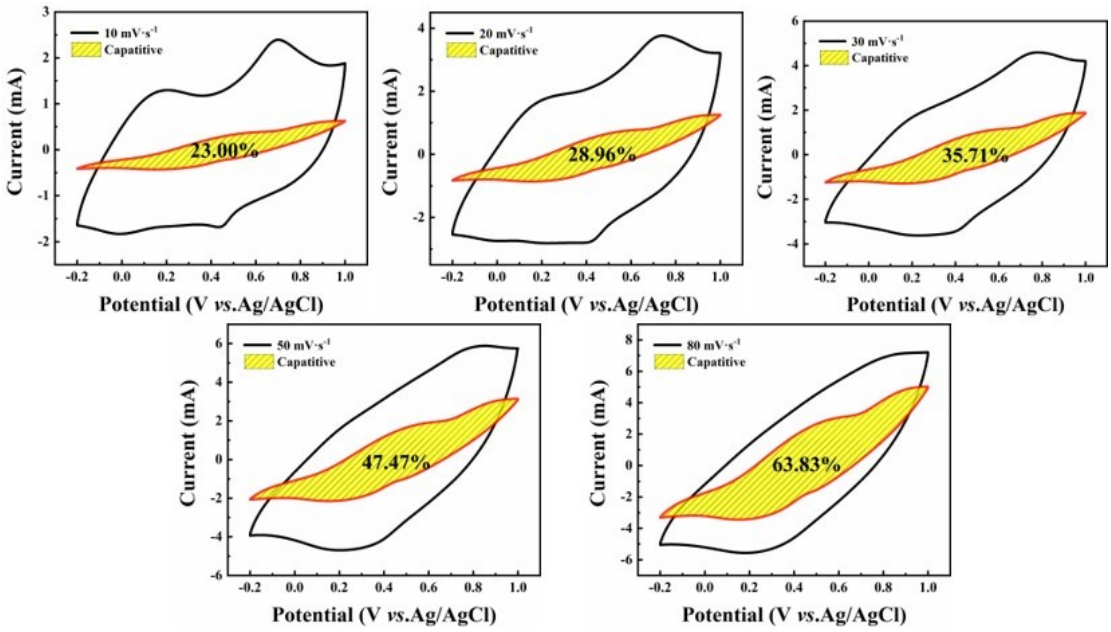

Fig. S9. Pseudocapacitive fraction (shown by the shaded area) calculated at a scan rate of 10-80 mV s^{-1} from CV curves at different scan rates of δ-MnO_2 electrode.

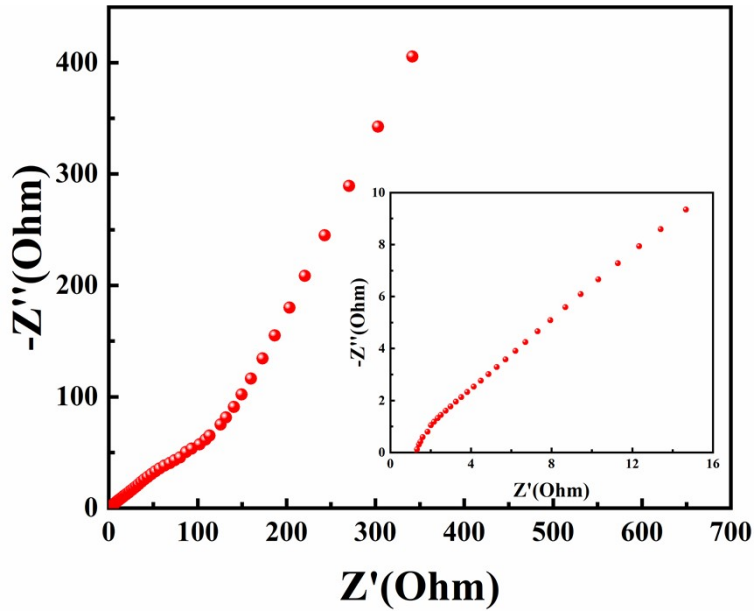

Fig. S10. Nyquist plots of A-MnO_2//La-MoO_3/GQD ASC device (inset: the Nyquist plots magnified at high frequencies).

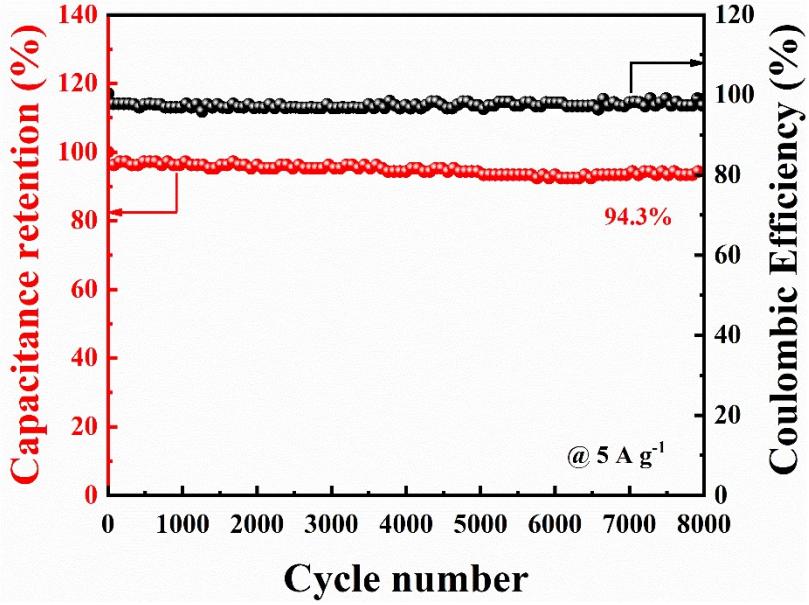

Fig. S11. Long cyclic stability tests for 8,000 cycles of A-MnO_2//La-MoO_3/GQD.

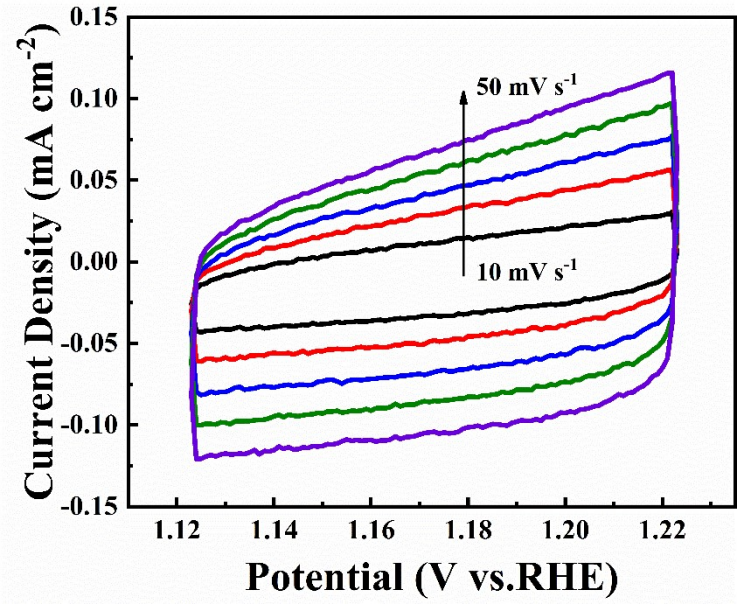

Fig. S12. CV curves in the non-Faraday interval with different scan rates of δ-MnO_2.

Table S1. Ratio of Mn^{3+}/Mn^{4+} and O species content (at. %) obtained from XPS spectra of O 1s.

Sample	**Mn^{3+}/Mn^{4+}**	**Mn-O-Mn**	**Mn-O-H**	**H-O-H**
δ-MnO_2	1.84	61.8%	23.2%	15.0%
0.5 M-A-MnO_2	2.86	60.9%	25.9%	13.1%
1 M-A-MnO_2	3.25	49.2%	31.1%	19.6%
2 M-A-MnO_2	3.11	59.4%	29.5%	10.9%

Table S2. Specific surface area and pore characteristics of the C-A-MnO_2.

Sample	Surface Area (m^2 g^{-1})	Pore Diameter (nm)	Pore Volume (cm^3 g^{-1})
δ-MnO_2	91.043	3.824	0.481
0.5 M-A-MnO_2	158.740	3.815	0.824
1 M-A-MnO_2	372.344	3.814	1.786
2 M-A-MnO_2	157.777	3.814	0.804

Table S3. Comparison of electrochemical properties of A-MnO_2 samples.

Electrode	**Specific capacitance ($F\ g^{-1}$)**	**Electrolyte**	**Current density**	**Ref.**
MnO_2-R	181.70	1 M Na_2SO_4	0.5 A g^{-1}	[1]
CuO/MnO_2	228.00	1 M Na_2SO_4	0.25 A g^{-1}	[2]
MnO_2-b	212.68	0.5 M Na_2SO_4	3 mA cm^{-2}	[3]
MnOx-CM	224.60	1 M Na_2SO_4	0.2 A g^{-1}	[4]
D-MnO_2	202.00	1 M Na_2SO_4	1 A g^{-1}	[5]
MnO_2/La_2O_3	245.40	1 M Na_2SO_4	0.3 A g^{-1}	[6]
C/MnO_2	128.75	1 M Na_2SO_4	0.5 A g^{-1}	[7]
MnO_2-1H	222.50	1 M Na_2SO_4	0.5 A g^{-1}	[8]
1 M-A-MnO_2	252.20	1 M Li_2SO_4	0.5 A g^{-1}	This work

Table S4. Literature data on OER activity of MnO_2-based electrocatalysts.

Catalysts	**Electrolyte**	**Tafel slope (mV dec^{-1})**	**η(mV)@*j* (mA cm^{-2})**	**Ref.**
Co_3O_4-MnO_2-CNT	0.1 M KOH	66	420@10	[9]
α-MnO_2-NWN	1 M KOH	65.6	467@10	[10]
α-MnO_2	1 M KOH	87.7	490@10	[11]
β-MnO_2	1 M NaOH	90	550@10	[12]
Ni-MnO_2	0.1 M KOH	86	445@10	[13]
Al-MnO_2	1 M KOH	107.9	390@10	[14]
Fe-MnO_2	1 M KOH	158.1	449@10	[14]
1 M-A-MnO_2	1 M KOH	61	361@10	This work

References

[1] D. Zhang, J. Dai, J. Zhang, Y. Zhang, H. Liu, Y. Xu, J. Wu, P. Li, *ACS Omega* **2024**, *9*, 18032-18045.

[2] Z. Zhang, C. Ma, M. Huang, F. Li, S. Zhu, C. Hua, L. Yu, H. Zheng, X. Hu, Y. Zhang, *Journal of Materials Science: Materials in Electronics* **2015**, *26*, 4212-4220.

[3] W. Yang, H. Eraky, C. Zhang, A. P. Hitchcock, I. Zhitomirsky, *Chemical Engineering Journal* **2024**, *483*, 149391.

[4] L. Ding, Z. Li, L. Chen, Z. Qi, *Electrochimica Acta* **2023**, *455*, 142424.

[5] Y.-P. Zhu, C. Xia, Y. Lei, N. Singh, U. Schwingenschlögl, H. N. Alshareef, *Nano Energy* **2019**, *56*, 357-364.

[6] Y. Li, B. Guan, A. Maclennan, Y. Hu, D. Li, J. Zhao, Y. Wang, H. Zhang, *Electrochimica Acta* **2017**, *241*, 395-405.

[7] P. Li, J. Wu, L. Tang, H. Liu, Y. Xu, D. Zhang, *Ionics* **2023**, *29*, 3629-3639.

[8] K. O. Oyedotun, A. A. Mirghni, O. Fasakin, D. J. Tarimo, B. A. Mahmoud, N. Manyala, *Journal of Energy Storage* **2021**, *36*, 102419.

[9] D. Ye, T. Wu, H. Cao, Y. Wang, B. Liu, S. Zhang, J. Kong, *RSC Advances* **2015**, *5*, 26710-26715.

[10] Y. Chen, S. Yang, H. Liu, W. Zhang, R. Cao, *Chinese Journal of Catalysis* **2021**, *42*, 1724-1731.

[11] Y. Meng, W. Song, H. Huang, Z. Ren, S.-Y. Chen, S. L. Suib, *Journal of the American Chemical Society* **2014**, *136*, 11452-11464.

[12] M. Fekete, R. K. Hocking, S. L. Y. Chang, C. Italiano, A. F. Patti, F. Arena, L. Spiccia, *Energy & Environmental Science* **2013**, *6*, 2222-2232.

[13] K. Bera, A. Karmakar, K. Karthick, S. S. Sankar, S. Kumaravel, R. Madhu, S. Kundu, *Inorganic Chemistry* **2021**, *60*, 19429-19439.

[14] H. Sun, S. Chen, B. Zhang, J. Wang, J. Yao, D. Li, G. Yuan, *Dalton Transactions* **2023**, *52*, 17407-17415.